Investigation of the Working Principle in an Optically Coupled Hot-Carrier Solar Cell Using the Relaxation-Time Model

J. Yang,* R. Patterson, Y. Feng, S. Shrestha, S. Huang, and G. Conibeer

Australian Centre for Advanced Photovoltaics, UNSW Australia, Sydney, New South Wales 2052, Australia

(Received 24 December 2014; published 14 April 2015)

Strong optical coupling is a carrier extraction method for hot-carrier solar cells, where carriers are extracted as photons from an absorber material and then reabsorbed by a conventional photovoltaic (PV) cell. The design and working principle of this kind of optically coupled device is investigated using a relaxation-time model with practical operating conditions. This investigation is performed in the so-called "down-conversion" configuration, where the band gap of the absorber material is the same as that in the final photovoltaic cell. In this configuration, carrier impact ionization rates that are faster than thermalization rates by at least 50 times are needed to effectively down-convert the hot carriers' energy to the electronic band edge. Photon emission through radiative recombination must be enhanced by more than 500 times through photonic engineering in order to reduce Auger loss during carrier extraction. The strong luminescence from the PV cell feeding back to the absorber material will further limit the optical extraction in the near-field coupled structure, reducing the overall conversion efficiency to be lower than the ideal expectation reported previously. The strong similarity between the hot-carrier down-conversion and carrier multiplication also suggests the possible application of such optical extraction for multiple-exciton-generation solar cells, making it potentially a general carrier extraction approach for third-generation solar cells.

DOI: 10.1103/PhysRevApplied.3.044006

I. INTRODUCTION

Conventional single-junction photovoltaic devices suffer from several fundamental energy-loss mechanisms such that their conversion efficiency cannot exceed the Shockley-Queisser limit. One of these losses occurs when the device is illuminated by the broadband solar spectrum, where most of the kinetic energy contained in the photoexcited carriers will be dissipated to the lattice as heat during carrier relaxation to the respective band edges. This thermalization loss is caused by inelastic carrier scattering and has a typical time scale of several picoseconds. Hot-carrier solar cells (HCSCs) with energy-selective contacts (ESCs) are designed to extract hot carriers before they are fully thermalized and, therefore, reduce the energy dissipation to the lattice [1,2]. The predicted limit to the efficiency can be as high as 85.4% [1], which is essentially the black-body limit for photovoltaic conversion [3]. However, inelastic scattering during electronic transport and the finite width of the energy-extraction window dramatically increase the energy loss inside an ESC structure [4,5]. Nanostructured absorbers will also likely suffer from reduced electrical conductivity and defect-assisted nonradiative recombination in both the all-optical and conventional hot-carrier [6–9] solar-cell approaches. These restrictions make it challenging to fabricate HCSC devices with ideal electrical performance.

Recently, an optical carrier extraction strategy has been proposed [10]. In this approach, the radiative recombination of hot carriers at specific energy levels in the absorber is artificially enhanced using a photonic structure, leading to an optical energy-selective contact (OESC). The emitted photons will be reabsorbed by a near-field coupled conventional photovoltaic (PV) cell that has a band gap matching exactly with the photon energy. Solely from a thermodynamic point of view, no extra entropy is produced within this photonic operation as long as the radiative energy transfer is reversible, which requires an infinitesimal extraction window with infinite available optical modes [11]. This optical approach can also be understood as a carrier-induced spectrum up- or down-conversion [12–14] and shows significant potential for application to conventional PV cells. Attractive results with efficiency figures over 60% have been predicted in the first estimation [10]. However, the effects of thermalization and carrier recombination losses have not yet been explored in detail, and these mechanisms are known to have a significant impact on the device performance.

In order to consider this optically coupled PV device in more detail, a relaxation-time model (RTM) [15] with experimentally achievable material parameters is used to predict device performance with optical carrier extraction. In the RTM, the final steady state of the system is determined by iterations in the time domain; therefore, the energy loss due to nonideal factors can be considered

*jianfeng.yang@student.unsw.edu.au

through the competition between different carrier evolution mechanisms. The conditions required for an effective optical extraction and device efficiency enhancements can be shown considering practical working parameters. A precisely engineered photonic structure is placed between the hot-carrier absorber and a PV cell to act as an OESC. This structure can be a Purcell cavity. The optical modes supported by a Purcell cavity increase the local optical density of states between the absorber and PV cell near the resonant frequency, therefore, accelerating the radiative recombination of electron-hole pairs [16,17]. The enlarged optical density of states can also strongly concentrate the electromagnetic field in a near-field region and enhance the photon absorption of the PV cell [18].

II. THEORETICAL MODEL

It is of interest to explore this down-conversion configuration further, where the absorber and PV cell share the same band gap, since an ultrahigh conversion efficiency has been predicted for this design. Different from the traditional HCSC concept, where the difference in the extraction energies for electrons and holes is larger than the band gap, the PV cell discussed here is working at its band edge. Therefore, in order to acquire an increased conversion efficiency, the actual photon flux absorbed by the PV cell must be increased, which requires a gain in the photon's number during the initial absorption and fast radiative reemission process. This particle gain can be provided only by the impact ionization of hot carriers in the absorber, as illustrated in Fig. 1. As assumed in Ref. [10], the hot-carrier gas has ideal zero thermalization loss and other nonradiative recombination loss in the absorber. Energy conversion at an energy below the carriers' average energy (the band gap of material) naturally leads the carrier multiplication. That the carriers have zero chemical potential provided by infinitely fast impact ionization and Auger recombination (AI), also gives the largest freedom to change the number of carriers to balance energy fluxes. This condition is responsible for the effective carrier multiplication in previous work. In the thermodynamic view, the carrier multiplication can also utilize the extra kinetic energy of hot carriers and reduce the thermalization loss, which is very similar to the multiple-exciton-generation (MEG) concept [19,20]. However, in a practical situation, inevitably thermalization loss will reduce the total amount of energy that could be converted by impact ionization. The reciprocal Auger recombination process will also consume newly created carriers at the band edge that might become photons flowing to the PV cell.

The modeling process is centered on the evaluation of the carrier distribution in the photon absorber. A nonequilibrium carrier distribution will relax to the corresponding equilibrium distribution exponentially within the relaxation time. Therefore, the transition increment for electrons in the photon absorber

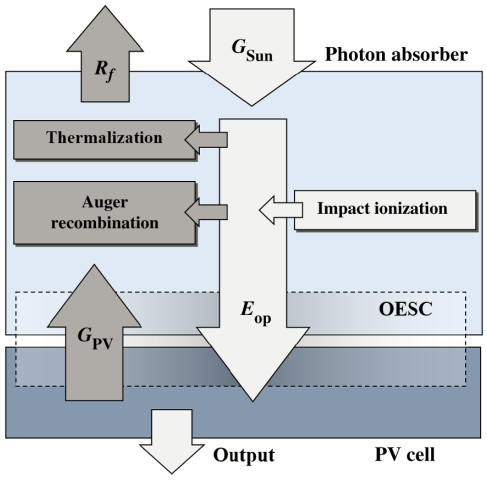

FIG. 1. Schematic illustration of the optically coupled hot-carrier solar cell in the down-conversion configuration. G_{Sun}, G_{PV}, R_f, and E_{op} represent photon generation by the incident light from the Sun, photon generation by the luminescence from the PV cell, photons returned to the Sun, and optical extraction to the PV cell, respectively. The photon absorber absorbs the incident light and pumps the photons to a PV cell with an identically matching band gap. An OESC provides a selective optical coupling between the photon absorber and PV cell at the band edge and inhibits the photon exchange at other frequencies in an ideal case. Both the thermalization and Auger recombination will cause energy loss in the down-conversion configuration, while impact ionization can be seen as a gain mechanism to the final conversion efficiency. All these carrier processes will compete with each other in real time to determine the final output.

$\Delta n(t)/\Delta t$ at electron energy level ε_e above the band edge can be represented as

$$\frac{\Delta n(t,\varepsilon_e)}{\Delta t} = -\frac{n(\varepsilon_e,t)-n_{\text{eq-}ee}(\varepsilon_e)}{\tau_{ee}} - \frac{n(\varepsilon_e,t)-n_{\text{eq-}eh}(\varepsilon_e)}{\tau_{eh}} - \frac{n(\varepsilon_e,t)-n_{\text{eq-th}}(\varepsilon_e)}{\tau_{\text{th}}} - \frac{n(\varepsilon_e,t)-n_{\text{eq-AI}}(\varepsilon_e)}{\tau_{\text{AI}}} + G_{\mathrm{Sun}}(\varepsilon_e) + G_{\mathrm{PV}}(\varepsilon_e) - R_f(\varepsilon_e) - E_{\mathrm{op}}(\varepsilon_e). \quad (1)$$

In Eq. (1), τ_{ee}, τ_{eh}, τ_{th}, τ_{AI} are the relaxation times for electron-electron scattering, electron-hole scattering, thermalization, and Auger recombination and impact ionization (AI), respectively. The $n_{\text{eq-}X}$ in Eq. (1) represents the corresponding thermodynamic equilibrium distributions for every kind of carrier process, which are determined by the same method used in Ref. [15]. A similar equation holds for the distribution of holes. Auger recombination and impact ionization have the same relaxation time τ_{AI}, and the overall effect of these two reciprocal processes drives the electrochemical potential of electron-hole pairs to zero [2]. $G_{\mathrm{Sun}}(\varepsilon_e)$, $G_{\mathrm{PV}}(\varepsilon_e)$, $R_f(\varepsilon_e)$, and $E_{\mathrm{op}}(\varepsilon_e)$ are the rates of photon generation by the incident photons from

the Sun, photon generation by the luminescence from the PV cell, photons returned to the Sun, and optical extraction to the PV cell, respectively, as shown in Fig. 1. The incident photons are assumed to be absorbed completely by the photon absorber with a thickness d of 50 nm, the same as in previous work [5,15,21], and the photon-generation rate from the carrier concentration is given by Eq. (2). The concentration ratio R_c is set to 1000 to ensure that there is enough hot-carrier excitation [22], and the term $j_{\mathrm{Sun}}[E_g + (1 + m_h^*/m_e^*)\varepsilon_e]$ represents the one-sun photon flux spectrum written in terms of the electron energies. The term $E_g + (1 + m_h^*/m_e^*)\varepsilon_e$ in the square bracket emphasizes that the photon flux is calculated by the corresponding photon's energy level, starting from the band gap E_g. A parabolic band structure characterized by the electron's and hole's effective mass (m_e^*, m_h^*) is used here, and only the direct absorption transition is considered. Momentum is conserved when the electron's energy is converted to the corresponding photon energy during the intraband carrier transition. The radiative recombination rate of the carriers at a particular density back to the Sun follows the generalized Plank's law, and both the actual distribution (n, h) and density of states (ρ_e, ρ_h) of electrons and holes are taken into account as shown in Eq. (3):

$$G_{\mathrm{Sun}}(\varepsilon_e) = R_c j_{\mathrm{Sun}}[E_g + (1 + m_h^*/m_e^*)\varepsilon_e]/d, \tag{2}$$

$$R_f(\varepsilon_e) = \frac{1}{d}\frac{2\pi}{h^3c^2}\frac{[E_g + (1 + m_h^*/m_e^*)\varepsilon_e]^2}{[\rho_e(\varepsilon_e)/n(\varepsilon_e) - 1]\{[\rho_h(\varepsilon_e m_h^*/m_e^*)/h(\varepsilon_e m_h^*/m_e^*) - 1]\} - 1}. \tag{3}$$

The photon flux between the absorber and the PV cell must be enhanced by the OESC structure in order to make the photonic transport as effective as the electronic one. The local density of photonic states within the OESC structure will be enlarged, and, therefore, the internal spontaneous emission rate of an excited dipole will be accelerated compared to the rate in a homogenous and isotropic photonic environment [17]. A rough estimation of the photon flux through the OESC is given by Eq. (4), where F represents the enhancement of the photon emission due to the Purcell cavity, and n_r is the refractive index of the material. The rectangular window function $W(\varepsilon_e)$ represents the simplified frequency selection imposed by the resonant Purcell cavity, where only a mode with a resonant wavelength can exist within the cavity and undergo accelerated spontaneous emission. In this down-conversion device, the resonant frequency corresponds to the identical band gap of both the photon absorber and PV cell. The effective width of the window function taken to be the full width at half maximum of the resonance peak will be characterized by the resonant frequency and quality factor Q of the system. The quality factor describes the energy-loss rate of the resonant mode, which is related to parasitic absorption loss and leaking processes,

$$E_{\mathrm{op}}(\varepsilon_e) = F n_r^2 R_f(\varepsilon_e) W(\varepsilon_e), \tag{4}$$

$$W(\varepsilon_e) = \begin{cases} 1, & 0 < \varepsilon_e < \frac{E_g m_h^*}{(m_e^* + m_h^*)Q}, \\ 0, & \text{otherwise.} \end{cases} \tag{5}$$

Similarly, electroluminescence from the PV cell will also be totally absorbed in the absorber material, and the evenly distributed photon-generation rate is

$$G_{\mathrm{PV}} = F W(\varepsilon_e) n_r^2 j_{\mathrm{BB}}[E_g + (1 + m_h^*/m_e^*)\varepsilon_e; 300\ \mathrm{K}; V]/d. \tag{6}$$

The $j_{\mathrm{BB}}[E_g + (1 + m_h^*/m_e^*)\varepsilon_e; 300\ \mathrm{K}; V]$ term is the black-body radiation at 300 K with a chemical potential equal to the working voltage (V) of the cell. The final conversion efficiency of the overall device under a specific optical concentration ratio R_c and total input power $P_{\mathrm{total}}(R_c)$ can be further represented as

$$\eta = \frac{V(E_{\mathrm{op}} - G_{\mathrm{PV}})d}{P_{\mathrm{total}}(R_c)}. \tag{7}$$

The calculation is initialized with an equilibrium carrier distribution in the photon absorber at 300 K. The carrier's distribution will be updated according to Eq. (1) until it reaches a final steady state. Here, the band gap of material is tuned from 0.4 to 1 eV. The effective mass of electrons and holes is constant at $0.05m_0$ and $0.5m_0$, respectively (m_0 is the intrinsic electron mass). This band gap and effective mass is similar to many of the potential III-V hot-carrier absorber materials [23]. The width of the extraction window is 0.02 eV, which means the quality factor is about 30. This number is the typical value of quality factor for plasmonic Purcell cavity where a spontaneous emission acceleration of over 1000 times has been successfully observed [24,25]. The hot-carrier thermalization time is assumed to be 100 ps here, which is a typical number chosen for hot-carrier solar cells [21,22,26,27]. For simplicity, a constant AI relaxation time for both impaction ionization and Auger recombination is used here, which is given as a ratio to the thermalization time to denote the competition between these two mechanisms. The highest rate of the AI process we consider is 200 fs, which is a typical time scale for this carrier process in a nanomaterial

[28–31]. It should be noted that the Auger loss may possibly be overestimated in this limiting case. A much slower Auger recombination compared to carrier multiplication has been observed in a large number of experiments where the lifetime of the Auger recombination is typically several tens to hundreds of picoseconds [28,30]. However, this overestimation will not affect the working principle discussed here.

III. RESULTS AND DISCUSSIONS

The conversion efficiency as a function of the band gap is given in Fig. 2. The conversion efficiency calculated in this work is much smaller than the previous estimation [10] due to energy loss. Figure 2 clearly shows that the conversion efficiency relies on the efficient optical extraction and rapid AI processes. The highest efficiency, about 29%, occurs when the band gap is close to 0.7 eV, and both the rate of the optical extraction and AI process are at their maximum. The inset in Fig. 2 shows the conversion efficiency of the device when the thermalization is set to the ideal case while the AI relaxation time is constant at 200 fs. A significant improvement of conversion efficiency can be observed when the thermalization time is increased to nanoseconds. An efficiency near 70% can be acquired when the thermalization is sufficiently long, which is in accordance with the prediction in Ref. [10].

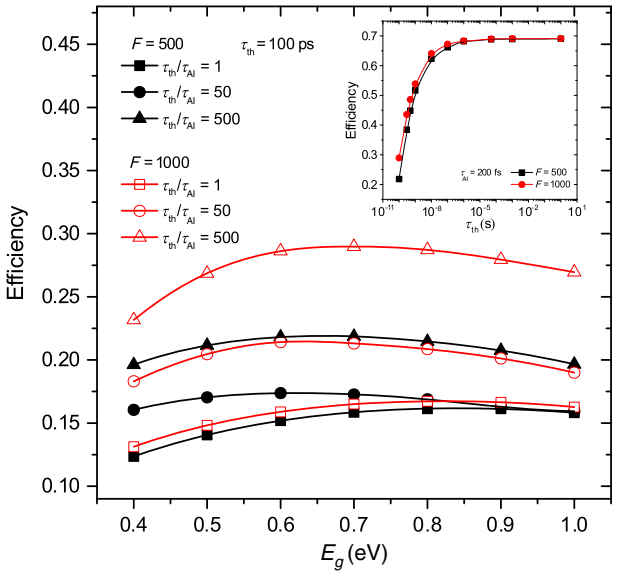

FIG. 2. Overall conversion efficiency of the optically coupled solar cell under different absorbers and PV cells. F is the emission enhancement factor representing the enhancement of the radiative lifetime. The thermalization time is constant at 100 ps while relaxation time of the AI process is given as a ratio to the thermalization time. The inset shows the efficiency when the thermalization time is sufficiently long and the AI relaxation lifetime is 200 fs. Over 60% conversion efficiency can be achieved when the thermalization time is similar to 10 ns.

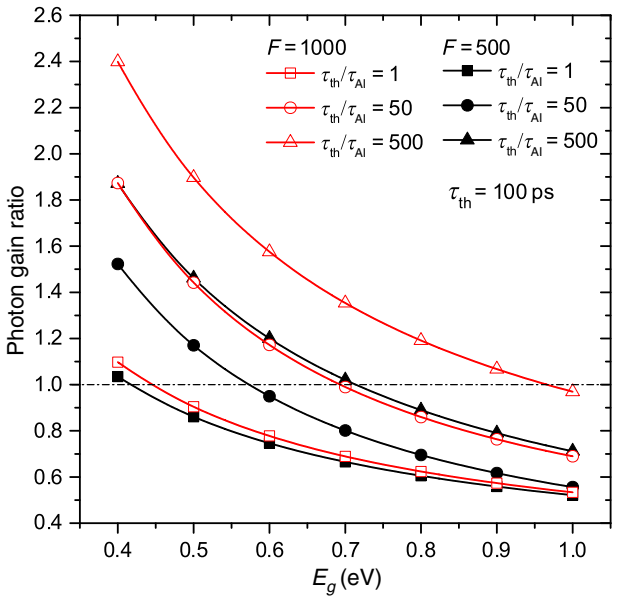

FIG. 3. Both the fast AI process and effective optical extraction can enlarge the actual photon flux leaving the absorber. With increasing absorber band gap, E_g, the net photon gain reduces and eventually becomes smaller than 1 under all the configurations.

As mentioned before, the efficiency enhancement in this down-conversion device comes from the enlarged photon flux delivered to the PV cell. Figure 3 shows the photon gain ratio in the photon absorber under different conditions. The photon gain ratio is defined as the output photon number from the absorber to the PV cell over the number of absorbed photons from the Sun, with the working voltage of the PV cell is kept at 0 V. Because the absorber and PV cell have the same band gap, the photon flux absorbed by the absorber is identical to the input photon current of the PV cell in the conventional case if an ideal absorption is assumed in both situations. Therefore, in order to obtain an increased conversion efficiency, the photon gain ratio must be larger than 1. Both the fast AI process and effective optical extraction can enlarge the actual photon flux leaving the absorber. For a constant carrier multiplication and extraction, the band gap of the material will modify the maximum absorbed energy. Similar to the considerations for MEG solar cells, a narrow band-gap material will have a higher gain ratio but suffers from a smaller open-circuit (OC) voltage [20]. Therefore, an optimized efficiency appears when varying the band gap in Fig. 2. This tendency reflects the trade-off between the output current and voltage in the device. Additionally, since the carrier gas in the photon absorber works at a temperature larger than 300 K, the radiative recombination loss back to the Sun will also be enlarged in this case. A much larger photon gain ratio is required here to maintain a high conversion efficiency for the device.

It is worth noticing the nonlinear dependence between F and the photon gain ratio in Fig. 3, where the actual photon

gain ratio is smaller than 2 when F is increased from 500 to 1000. According to Eqs. (3) and (4), we calculate the carrier radiative recombination rate considering the actual distribution of carriers. The reduced photon emission reflects the nonideal carrier refilling in the photon absorber due to carrier-carrier scattering and AI processes. In Fig. 3, the photon gain ratio increases with the τ_{th}/τ_{AI} when F is doubled from 500 to 1000 due to the enhanced down-conversion rate contributing to faster refilling of empty electron states at the band edge. When $\tau_{th}/\tau_{AI} = 500$, the actual photon gain ratio shown in Fig. 3 is about 1.25. The actual photon emission will further affect the V_{OC} of the PV cell. Therefore, a nonlinear dependence between the conversion efficiency and F appears in Fig. 2.

A more detailed relationship for the photon gain ratio is shown in Fig. 4. The absorber's band gap is set to 0.7 eV here. It is necessary to emphasize that the gain in photon number is the result of carrier multiplication in the absorber by impact ionization as well as effective carrier extraction by radiative recombination. Hot carriers with elevated energy could potentially participate in impact ionization processes, a competing mechanism with thermalization. As a precondition for effective carrier multiplication, the rate of impact ionization should be faster than that for thermalization in order to take full advantage of a hot carrier's energy before it is thermalized. The ratio between the rates needs to be at least 50 times, as shown in Fig. 4. Carriers created by impact ionization may be Auger recombined without effective radiative recombination. Therefore, only with an efficient carrier extraction can the impact ionization dominate over Auger processes in the final steady state and make the photon gain ratio larger than 1. Otherwise, Auger recombination will cause severe particle loss. In this work, the required optical emission enhancement must be larger than about 500 times. This enhancement times is a major requirement for the OESC in this down-conversion configuration. Even when the impact ionization is not competitive with thermalization, where $\tau_{th}/\tau_{AI} < 50$, a rapid optical extraction rate can also reduce the Auger loss because of a reduced dwell time of newly created carriers at the band edge as well as the possibility for Auger recombination. In an extreme situation, if the carriers at the band edge are continuously depleted by extraction and carrier-carrier scattering is not quick enough to replenish

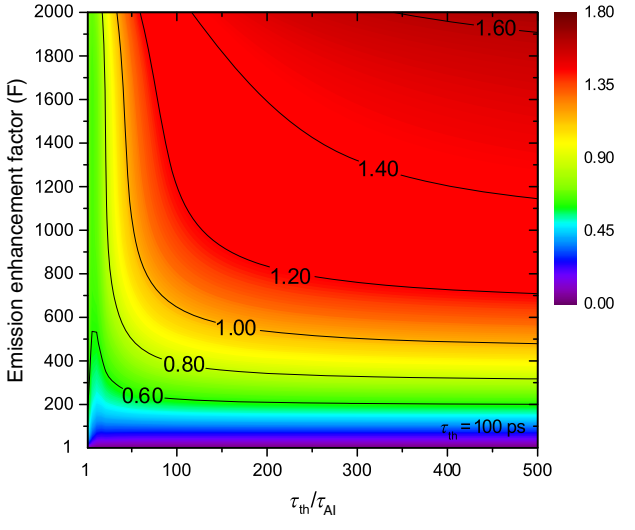

FIG. 4. The photon gain ratio under different emission enhancement and AI process rates. The lifetime of the AI process is presented as a ratio of the thermalization time of hot carriers. To get the photon gain, the required emission enhancement ratio should be larger than 500 times, and the AI process should be faster than carrier cooling by 50 times at least.

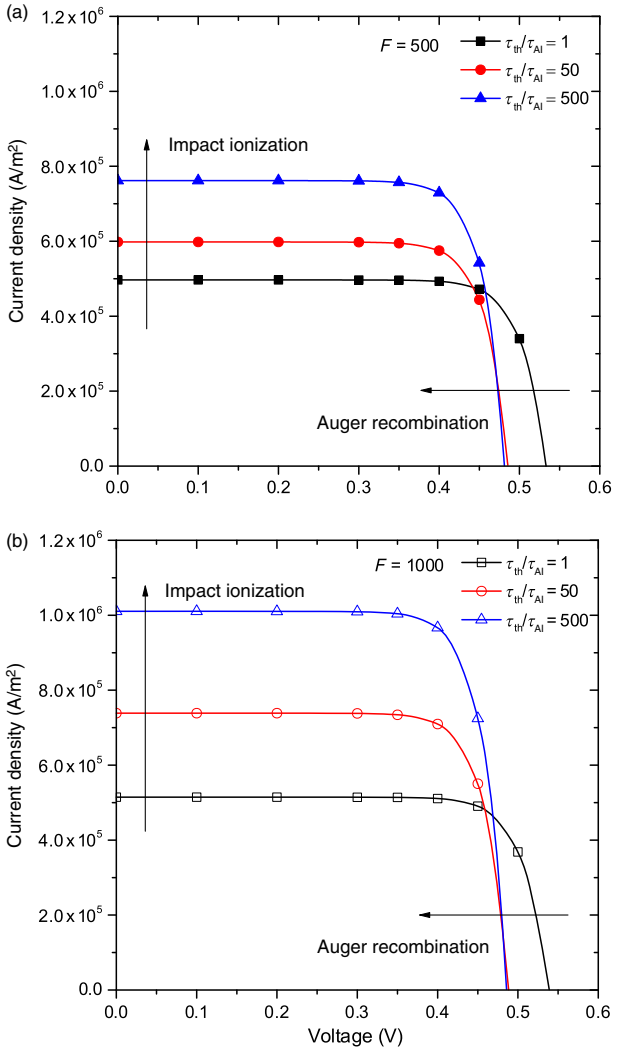

FIG. 5. *I-V* curve of a complete all-optical hot-carrier solar cell where the PV cell is closely attached to the top absorber, and a photonic structure is employed to provide spontaneous emission enhancement at a designated frequency. The band gap is 0.7 eV here. Two cases with an emission enhancement factor of 500 times (a) and 1000 times (b) are considered. Both figures show that a rapid AI process will increase the short-circuit current under a small working voltage but decrease the open-circuit voltage due to changes from AI processes.

them, rapid optical extraction can trigger more effective impact ionization in order to balance the thermal distribution of the charge carrier gas.

When the PV cell starts to generate current, the actual photon gain in the absorber will be smaller than when the PV cell is not biased. This decrease is reflected by the *I-V* curve of PV cell in the Fig. 5. When AI processes are rapid, the short-circuit current of the cell is significantly increased due to effective carrier multiplication. However, a decrease in the PV cell's open-circuit voltage is evident at the same time. Since the recombination loss of the PV cell is not changed, this drop of V_{OC} reflects the decrease in photon flux from the absorber material, which further indicates increased Auger recombination loss. In fact, the electroluminescence emitted by the PV cell will also excite carriers to the position just above the band edge of the photon absorber. This feedback electroluminescence through the same energy levels provided by the OESC will reduce the actual photon flux leaving the photon absorber to the PV cell. Therefore, the effective residence time of carriers at the band edge and the amount of Auger recombination is increased. From a carrier dynamics point of view, these carriers injected at the band edge will quench the hot-carrier distribution in the absorber and lead to unfavorable conditions for impact ionization. When the working voltage of the PV cell is close to V_{OC}, this feedback electroluminescence will strongly reduce the yield from carrier multiplication in the absorber. This mechanism further limits the actual enlargement of the overall conversion efficiency as calculated in Fig. 2 compared to the photon gain ratio showed in Fig. 3 where the PV cell is in the short-circuit condition.

IV. CONCLUSIONS

In this paper, the working principle of the down-conversion optically coupled hot-carrier solar cell is demonstrated in some detail. Based on the RTM method, the competition between dynamical carrier processes is assessed and energy loss caused by thermalization and Auger recombination is explicitly taken into account. The optical coupling concept still shows potential when subjected to a more practical estimation of its performance. The operation of this down-conversion hot-carrier device almost relies entirely on carrier multiplication through impact ionization, which strongly resembles a MEG solar cell. The competition between carrier thermalization and multiplication has been addressed in highly efficient MEG materials recently [32,33]. Effective optical extraction can also reduce the loss of newly created carriers at the band edge due to Auger recombination and other nonradiative recombination processes. Therefore, a similar device performance is predicted in an "optically coupled MEG solar cell." This similarity suggests a widespread potential application of this optical extraction approach in third-generation PV concepts, and only the extraction energy level would be tuned for a specific situation. Importantly, most of the third-generation PV materials are based on nanocrystals. Using optical extraction may possibly avoid problems caused by poor electronic transport and improve device performance. An asymmetric relaxation time for different phases of AI processes can be considered by introducing a carrier concentration and energy-dependent relaxation time $\tau_{AI}(n, h; \varepsilon)$ in future modeling in order to provide an increasingly accurate result. Considering the modified photonic environment in the Purcell cavity, a more detailed optical calculation would also be useful to better estimate the actual photon flux flowing to the PV cell. Both of these aspects are the subject of future work.

ACKNOWLEDGMENTS

This program is supported by the Australian government through the Australian Renewable Energy Agency. J. Y. thanks the China Scholarship Council (Scholarship No. 201306070023) for scholarship support. Responsibility for the views, information, or advice expressed herein is not accepted by the Australian Government.

[1] R. T. Ross and A. J. Nozik, Efficiency of hot-carrier solar energy converters, J. Appl. Phys. **53**, 3813 (1982).
[2] P. Würfel, Solar energy conversion with hot electrons from impact ionisation, Sol. Energy Mater. Sol. Cells **46**, 43 (1997).
[3] D. V. A., *Endoreversible Thermodynamics of Solar Energy Conversion* (Oxford University Press, Oxford, 1992).
[4] P. Aliberti, Y. Feng, S. Shrestha, M. Green, G. Conibeer, L. Tu, P. Tseng, and R. Clady, Effects of non-ideal energy selective contacts and experimental carrier cooling rate on the performance of an indium nitride based hot carrier solar cell, Appl. Phys. Lett. **99**, 223507 (2011).
[5] Y. Feng, P. Aliberti, B. P. Veettil, R. Patterson, S. Shrestha, M. A. Green, and G. Conibeer, Non-ideal energy selective contacts and their effect on the performance of a hot carrier solar cell with an indium nitride absorber, Appl. Phys. Lett. **100**, 053502 (2012).
[6] A. Pandey and P. Guyot-Sionnest, Hot electron extraction from colloidal quantum dots, J. Phys. Chem. Lett. **1**, 45 (2010).
[7] M. L. Mueller, X. Yan, B. Dragnea, and L. S. Li, Slow hot-carrier relaxation in colloidal graphene quantum dots, Nano Lett. **11**, 56 (2011).
[8] A. J. Nozik, M. C. Beard, J. M. Luther, M. Law, R. J. Ellingson, and J. C. Johnson, Semiconductor quantum dots and quantum dot arrays and applications of multiple exciton generation to third-generation photovoltaic solar cells, Chem. Rev. **110**, 6873 (2010).
[9] A. Pandey and P. Guyot-Sionnest, Slow electron cooling in colloidal quantum dots, Science **322**, 929 (2008).
[10] D. J. Farrell, Y. Takeda, K. Nishikawa, T. Nagashima, T. Motohiro, and N. J. Ekins-Daukes, A hot-carrier solar cell

with optical energy selective contacts, Appl. Phys. Lett. **99**, 111102 (2011).
[11] A. Devos and H. Pauwels, Comment on a thermodynamical paradox presented by Wurfel, Peter, J. Phys. C **16**, 6897 (1983).
[12] T. Trupke, M. A. Green, and P. Wurfel, Improving solar cell efficiencies by down-conversion of high-energy photons, J. Appl. Phys. **92**, 1668 (2002).
[13] B. S. Richards, Luminescent layers for enhanced silicon solar cell performance: Down-conversion, Sol. Energy Mater. Sol. Cells **90**, 1189 (2006).
[14] A. Shalav, B. S. Richards, and M. A. Green, Luminescent layers for enhanced silicon solar cell performance: Up-conversion, Sol. Energy Mater. Sol. Cells **91**, 829 (2007).
[15] Y. Feng, R. Patterson, S. Lin, S. Shrestha, S. Huang, M. Green, and G. Conibeer, Investigation of carrier-carrier scattering effect on the performance of hot carrier solar cells with relaxation time approximation, Appl. Phys. Lett. **102**, 243901 (2013).
[16] E. Purcell, Proceedings of the American Physical Society, Phys. Rev. **69**, 674 (1946).
[17] M. Boroditsky, R. Vrijen, T. F. Krauss, R. Coccioli, R. Bhat, and E. Yablonovitch, Spontaneous emission extraction and Purcell enhancement from thin-film 2-D photonic crystals, J. Lightwave Technol. **17**, 2096 (1999).
[18] S. Basu, Z. Zhang, and C. Fu, Review of near-field thermal radiation and its application to energy conversion, Int. J. Energy Res. **33**, 1203 (2009).
[19] A. J. Nozik, Quantum dot solar cells, Physica (Amsterdam) **14E**, 115 (2002).
[20] M. C. Hanna, M. C. Beard, and A. J. Nozik, Effect of solar concentration on the thermodynamic power conversion efficiency of quantum-dot solar cells exhibiting multiple exciton generation, J. Phys. Chem. Lett. **3**, 2857 (2012).
[21] P. Aliberti, Y. Feng, Y. Takeda, S. K. Shrestha, M. A. Green, and G. Conibeer, Investigation of theoretical efficiency limit of hot carriers solar cells with a bulk indium nitride absorber, J. Appl. Phys. **108**, 094507 (2010).
[22] Y. Takeda, T. Ito, T. Motohiro, D. Konig, S. Shrestha, and G. Conibeer, Hot carrier solar cells operating under practical conditions, J. Appl. Phys. **105**, 074905 (2009).
[23] D. König, K. Casalenuovo, Y. Takeda, G. Conibeer, J. Guillemoles, R. Patterson, L. Huang, and M. Green, Hot carrier solar cells: Principles materials and design, Physica (Amsterdam) **42E**, 2862 (2010).
[24] C. H. Cho, C. O. Aspetti, M. E. Turk, J. M. Kikkawa, S. W. Nam, and R. Agarwal, Tailoring hot-exciton emission and lifetimes in semiconducting nanowires via whispering-gallery nanocavity plasmons, Nat. Mater. **10**, 669 (2011).
[25] C. H. Cho, C. O. Aspetti, J. Park, and R. Agarwal, Silicon coupled with plasmon nanocavity generates bright visible hot-luminescence, Nat. Photonics **7**, 285 (2013).
[26] Y. Takeda, T. Motohiro, D. Konig, P. Aliberti, Y. Feng, S. Shrestha, and G. Conibeer, Practical factors lowering conversion efficiency of hot carrier solar cells, Appl. Phys. Express **3**, 104301 (2010).
[27] D. König, Y. Yao, and R. Patterson, Shortcomings in efficiency modelling of hot carrier solar cells: Considering device concepts and hot carrier absorber materials from a practical viewpoint, Jpn. J. Appl. Phys. **53**, 05FV04 (2014).
[28] R. J. Ellingson, M. C. Beard, J. C. Johnson, P. Yu, O. I. Micic, A. J. Nozik, A. Shabaev, and A. L. Efros, Highly efficient multiple exciton generation in colloidal PbSe and PbS quantum dots, Nano Lett. **5**, 865 (2005).
[29] R. D. Schaller, V. M. Agranovich, and V. I. Klimov, High-efficiency carrier multiplication through direct photogeneration of multi-excitons via virtual single-exciton states, Nat. Phys. **1**, 189 (2005).
[30] A. Franceschetti, J. M. An, and A. Zunger, Impact ionization can explain carrier multiplication in PbSe quantum dots, Nano Lett. **6**, 2191 (2006).
[31] Y. Fu, Y.-H. Zhou, H. Su, F. Y. C. Boey, and H. Ågren, Impact ionization and Auger recombination rates in semiconductor quantum dots, J. Phys. Chem. C **114**, 3743 (2010).
[32] V. I. Klimov, Multicarrier interactions in semiconductor nanocrystals in relation to the phenomena of Auger recombination and carrier multiplication, Annu. Rev. Condens. Matter Phys. **5**, 285 (2014).
[33] J. T. Stewart, L. A. Padilha, M. M. Qazilbash, J. M. Pietryga, A. G. Midgett, J. M. Luther, M. C. Beard, A. J. Nozik, and V. I. Klimov, Comparison of carrier multiplication yields in PbS and PbSe nanocrystals: The role of competing energy-loss processes, Nano Lett. **12**, 622 (2012).